

## Copper Corrosion Inhibition by Cefpodoxime Drug in 1M Nitric Acid : Experimental and DFT approaches

*OUEDRAOGO Augustin, DIKI N'guessan Yao Silvère, IRIE Bi Irié Williams, Coulibaly Nagnonta Hippolyte,  
and TROKOUREY Albert*

Laboratoire de Chimie Physique, Université Félix Houphouët-Boigny, 22BP 582 Abidjan 22, Côte d'Ivoire

Copyright © 2018 ISSR Journals. This is an open access article distributed under the **Creative Commons Attribution License**, which permits unrestricted use, distribution, and reproduction in any medium, provided the original work is properly cited.

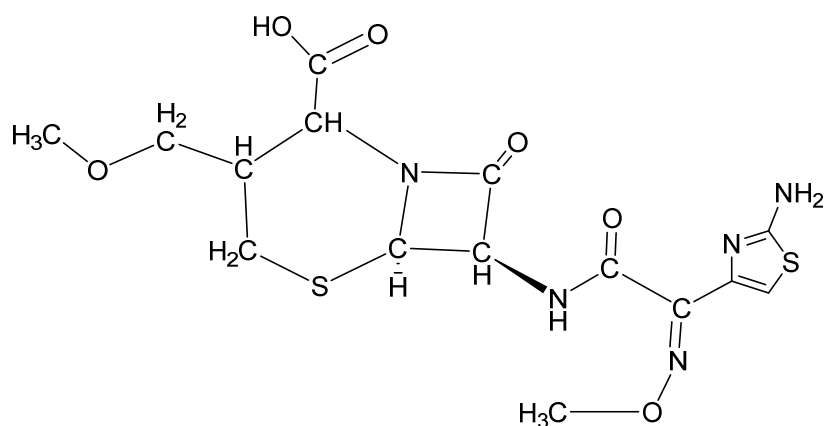
**ABSTRACT:** The copper corrosion inhibition in one molar nitric acid by cefpodoxime drug is studied via mass loss technique at 303-323K and quantum chemistry. The results show that the studied drug is an efficient inhibitor which adsorbs spontaneously on copper through Langmuir model. Thermodynamic adsorption functions and activation ones were determined and analyzed. They indicate a predominant physisorption process and an endothermic dissolution process. Scanning electron microscopy was used to characterize the metal surface. Quantum chemical calculations at B3LYP level with 6-31G (d, p) basis set lead to molecular descriptors such as  $E_{\text{HOMO}}$  (energy of the highest occupied molecular orbital),  $E_{\text{LUMO}}$  (energy of the lowest unoccupied molecular orbital),  $\Delta E$  (energy gap) and  $\mu$  (dipole moment). The global reactivity descriptors such as  $\chi$  (electronegativity),  $\eta$  (hardness),  $S$  (softness) and  $\omega$  (electrophilicity index) were derived using Koopman's theorem and analyzed. The local reactivity parameters including Fukui functions  $f(\vec{r})$  and local softness  $s(\vec{r})$  were determined and discussed. Theoretical results were found to be consistent with the experimental data.

**KEYWORDS:** Adsorption, mass loss, physisorption, Fukui functions, local softness.

### 1 INTRODUCTION

Copper is widely used [1, 2] due to its excellent corrosion resistance, mechanical, thermal and electrical conductivity properties. However, when being in contact with acids such as nitric acid during industrial stripping and other cleaning operations, it undergoes corrosion. The most practical method [3, 4] used to combat copper acid corrosion is the use of non-toxic organic corrosion inhibitors (e.g. addition of heterocyclic organic compounds in the metal's environment). Up to now, various organic compounds containing heteroatoms such as O, N and S have been reported to be good inhibitors for copper corrosion in nitric acid media. Indeed, it is generally accepted [5] that organic compounds exert their inhibitory action via adsorption on metal surface through the heteroatoms and their double bonds in the aromatic rings. The adsorption of the organic compounds onto the metal surface is influenced by their chemical structures.

The use of quantum chemical calculations [6] leads to structural and reactivity parameters of molecules. Many studies in the literature [7-9] have reported on the use of DFT calculations in copper acid corrosion inhibition. It is revealed that the inhibitory action of the organic compounds is correlated with the theoretical parameters such as the highest occupied molecular orbital energy ( $E_{\text{HOMO}}$ ), the lowest unoccupied molecular orbital energy ( $E_{\text{LUMO}}$ ), the energy gap  $\Delta E$ , the dipole moment  $\mu$ , the Mulliken atomic charges, etc. Actually, the choice of effective corrosion inhibitors [10, 11] is generally based on the correlation between experimental data (inhibition efficiency from mass loss or/ and electrochemical studies) and the quantum chemical properties (electron donating or/and accepting ability) of the studied molecules. In this work, the inhibitory effect of cefpodoxime drug (**Scheme 1**) on copper corrosion in 1 M  $\text{HNO}_3$  solution is investigated by mass loss technique, scanning electron microscopy and quantum chemistry based on density functional theory (DFT), which is used to get insight into the corrosion inhibition mechanism.



Scheme 1: chemical structure of cefpodoxime

## 2 MATERIALS AND METHODS

### 2.1 COPPER SPECIMEN

The samples of copper used in this study were in the form of rods with 10 mm as length and 2.2 mm as diameter which were cut in commercial copper of purity 95%.

### 2.2 REAGENTS

Cefpodoxime of analytical grade with  $C_{15}H_{17}N_5O_6S_2$  as formula and acetone of purity 99.5% were purchased from Sigma-Aldrich Chemicals. Commercial nitric acid of purity 65% was purchased from Pan Reac AppliChem.

### 2.3 SOLUTION PREPARATION

1M  $HNO_3$  solutions without or with different concentrations of cefpodoxime ranging from 0.05 to 5mM were then prepared.

### 2.4 MASS LOSS METHOD

Before each measurement, the copper samples were mechanically abraded with different grade emery papers (1/0, 2/0, 3/0, 4/0, 5/0, and 6/0). The specimens were washed thoroughly with bidistilled water, degreased and rinsed with acetone and dried in an oven. Mass loss measurements were performed in a beaker of 100 mL capacity containing 50 mL of the test solution. The immersion time for mass loss was 1h at a given temperature. In order to get good reproducible data, parallel triplicate experiments were conducted accurately and the average mass loss was used to calculate the corrosion rate ( $W$ ), the degree of surface coverage ( $\theta$ ) and the inhibition efficiency (IE) using Equation 1-3 respectively:

$$W = \frac{m_1 - m_2}{St} \quad (1)$$

$$\theta = \frac{W_0 - W}{W_0} \quad (2)$$

$$IE(\%) = \left( \frac{W_0 - W}{W_0} \right) * 100 \quad (3)$$

where  $W_0$  and  $W$  are the corrosion rate without and with inhibitor respectively,  $m_1$  and  $m_2$  are the mass before and after immersion in the corrosive aqueous solution respectively,  $S$  is the total surface of the copper specimen and  $t$  is the immersion time.

### 2.5 SCANNING ELECTRON MICROSCOPY

The scanning electron microscopy (FEG SEM, SUPRA 40VP, ZEISS, Germany) was used to characterize the copper surface after its treatment in the presence or absence of cefpodoxime for 1 h immersion 303K. Comparison was made between the bare sample and the immersed ones.

## 2.6 QUANTUM CHEMICAL CALCULATIONS

To calculate the ground-state energy and the physical properties of cefpodoxime, the Gaussian 09 W package [12] was used. The molecular structure was optimized to a minimum without symmetry restrictions using B3LYP exchange correlation functional, a combination of the Becke three parameter hybrid functional [13] with the correlation functional of Lee, Yang and Parr [14, 15] associated to 6-31 G (d, p) basis set [16]. **Figure 1** presents the optimized structure of cefpodoxime. Density functional theory has been proved to be successful in providing theoretical basis for chemical concepts such as electronegativity ( $\chi$ ), hardness ( $\eta$ ), softness ( $S$ ) and local parameters as Fukui function ( $f(\vec{r})$ ), and local softness ( $s(\vec{r})$ ).

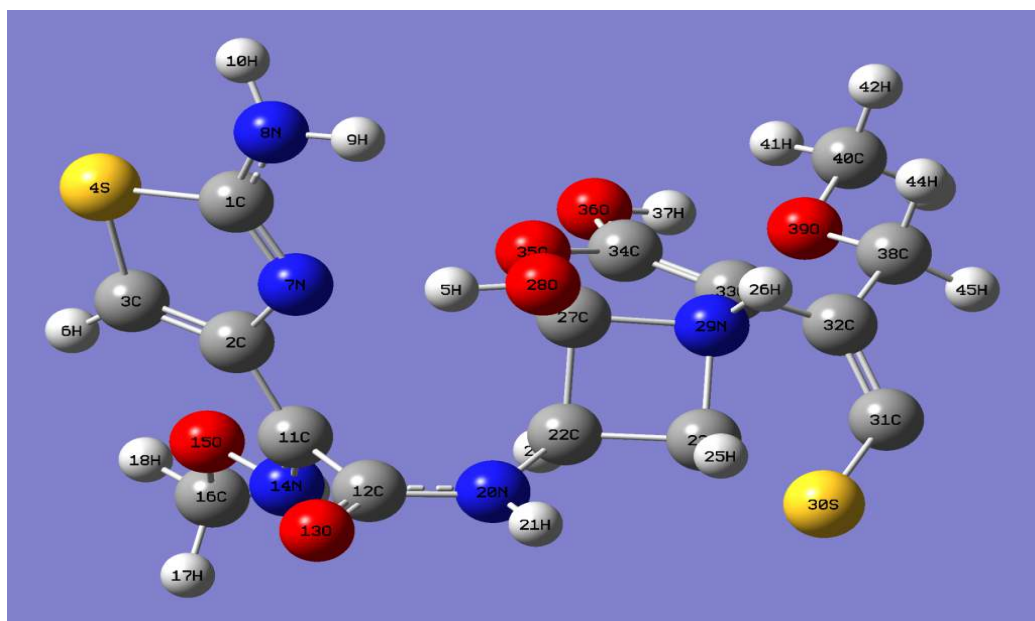


**Fig. 1.** Optimized structure of cefpodoxime by B3LYP/6-31G (d, p)

For N-electrons system with total energy E, the electronegativity is given by Equation 4:

$$\chi = -\mu_P = -\left(\frac{\partial E}{\partial N}\right)_{v(\vec{r})} \quad (4)$$

Where  $\mu_P$  and  $v(\vec{r})$  are the chemical and external potentials respectively. The chemical hardness  $\eta$  which is defined as the second derivative of E with respect to N is then given by Equation 5:

$$\eta = \left(\frac{\partial^2 E}{\partial N^2}\right)_{v(\vec{r})} \quad (5)$$

The global softness S is the inverse of the global hardness as seen in Equation 6:

$$S = \frac{1}{\eta} \quad (6)$$

According to Koopman's theorem [17], the ionization potential I can be approximated as the negative of the highest occupied molecular orbital (HOMO) energy:

$$I = -E_{HOMO} \quad (7)$$

The negative of the lowest unoccupied molecular orbital (LUMO) energy is related to the electron affinity A:

$$A = -E_{LUMO} \quad (8)$$

The electronegativity was obtained using the ionization energy I and the electron affinity A as given in Equation 9:

$$\chi = \frac{I+A}{2} \quad (9)$$

The hardness which is the reciprocal of the electronegativity was obtained by Equation 10:

$$\eta = \frac{I-A}{2} \tag{10}$$

When the organic molecule is in contact with the metal, electrons flow from the system with lower electronegativity to that of higher electronegativity until the chemical potential becomes equal. The fraction of electrons transferred,  $\Delta N$ , was estimated according to Pearson [18]:

$$\Delta N = \frac{\chi_{Cu} - \chi_{inh}}{2(\eta_{Cu} + \eta_{inh})} \tag{11}$$

In this study, we used theoretical values of  $\chi_{Cu}$  and  $\eta_{Cu}$  ( $\eta_{Cu} = 4.98$  eV) [19] and  $\eta_{Cu} = 0$  [20].

The global electrophilicity index, introduced by Parr [19] is given by Equation (12):

$$\omega = \frac{\chi^2}{2\eta} \tag{12}$$

The local selectivity of a corrosion inhibitor [21] is generally assessed using Fukui functions. Their values are used to identify which atoms in the inhibitor are more prone to undergo an electrophilic or nucleophilic attack. The change in electron density [22] is the nucleophilic and electrophilic Fukui functions, which are defined as:

$$f(\vec{r}) = \left( \frac{\partial \rho(\vec{r})}{\partial N} \right)_{v(\vec{r})} \tag{13}$$

1. where  $N$  and  $\rho(\vec{r})$  are the number of electrons and the electron density at position  $\vec{r}$  of the chemical species respectively. After taking care of the discontinuities in  $f(\vec{r})$  versus  $N$  plot, the “condensed-to-atom” approximations of  $f(\vec{r})$ , when multiplied by global softness ( $S$ ) [23] provide local softness values given by Equation 14-15 respectively:

$$s_k^+( \vec{r} ) = [q_k(N + 1) - q_k(N)]S = f_k^+ S \tag{14}$$

$$s_k^-( \vec{r} ) = [q_k(N) - q_k(N - 1)]S = f_k^- S \tag{15}$$

In these equations  $q_k(N + 1)$ ,  $q_k(N)$  and  $q_k(N - 1)$  represent the condensed electronic populations on atom “k” for anionic, neutral and cationic systems respectively. Therefore,  $s_k^+( \vec{r} )$  and  $s_k^-( \vec{r} )$  represent the condensed local softness values of atom “k” towards nucleophilic and electrophilic attacks.

### 3 RESULTS

#### 3.1 EFFECT OF TEMPERATURE AND CONCENTRATION ON CORROSION RATE

The corrosion rate curves of copper without and with the addition of cefpodoxime in 1M HNO<sub>3</sub> at different temperatures are shown in **Figure 2**. These curves reveal that corrosion rate of copper in the studied medium, increases with increasing temperature. But this evolution is moderated when the concentration of the studied compound increases.

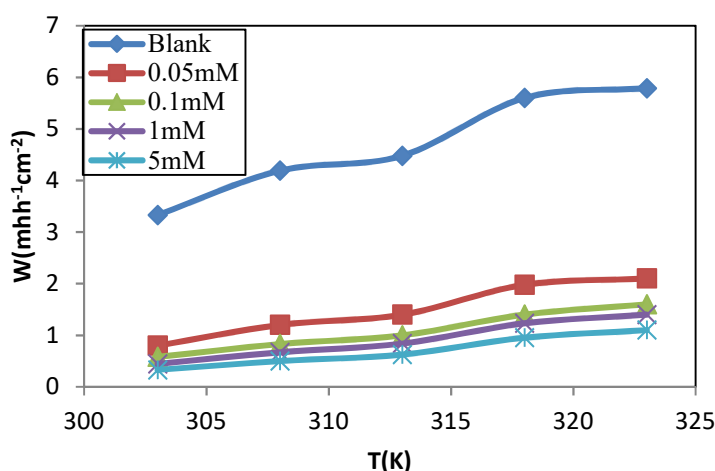


Fig. 2. Evolution of corrosion rate with temperature for different concentrations of cefpodoxime

For the temperature range studied, the inhibition efficiency (IE) increases with the increase in inhibitor concentration until a value of 90.09% for the concentration of 5 mM at 303K (Figure 3).

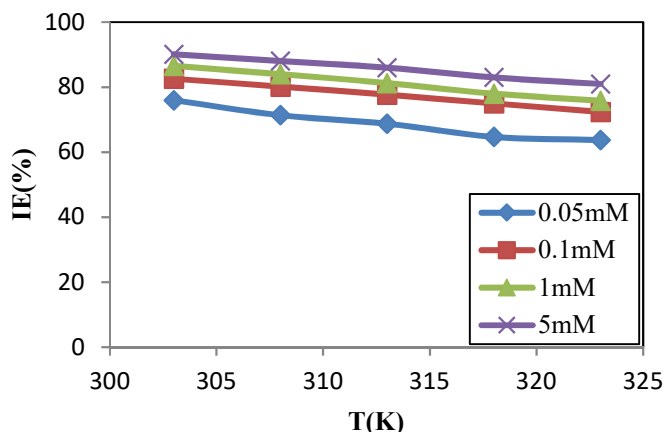


Fig. 3. Inhibition efficiency versus temperature for different concentrations of cefpodoxime

### 3.2 ADSORPTION ISOTHERMS

The basic information on the interaction between the inhibitor and the metal can be provided by the adsorption isotherm. The adsorption isotherms tested in this work are the models of Langmuir, Temkin, Freundlich, El-Awady and Flory Huggins. By fitting the degree of surface coverage ( $\Theta$ ) and the inhibitor concentration (Figure 4), the best adsorption isotherm obtained graphically is Langmuir adsorption isotherm with a strong correlation ( $R^2 > 0.999$ ) and the slopes of the straight lines are close to unity.

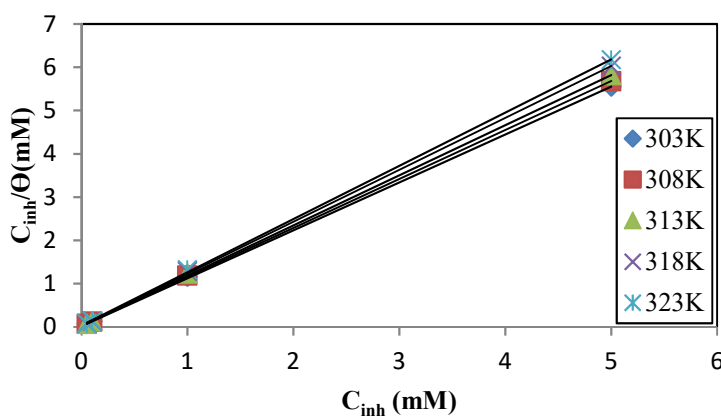


Fig. 4. Langmuir adsorption isotherm for cefpodoxime on copper surface in 1M HNO<sub>3</sub>

The obtained Langmuir adsorption parameters for different temperatures are presented in Table 1.

Table 1. Regression parameters of Langmuir isotherm

T(K)	Correlation coefficient	Slope	Intercept
303	1	1.1067	0.0214
308	0.9999	1.1315	0.0259
313	0.9999	1.1582	0.0308
318	0.9999	1.1994	0.0348
323	0.9998	1.2290	0.0374

3.3 THERMODYNAMIC ADSORPTION PARAMETERS

The calculated values of  $\Delta G_{ads}^0$  are presented in **Table 2**.

**Table 2. Thermodynamic parameters for the adsorption of cefpodoxime on copper surface at different temperatures.**

$T(K)$	$K_{ads}(M^{-1})$	$\Delta G_{ads}^0(kJ mol^{-1})$	$\Delta H_{ads}^0(kJ mol^{-1})$	$\Delta S_{ads}^0(J mol^{-1}K^{-1})$
303	46728.97	-37.19		
308	38610.04	-37.31		
313	32467.53	-37.47	-22.90	46.90
318	28735.63	-37.74		
323	26737.97	-38.14		

Thermodynamic adsorption parameters  $\Delta H_{ads}^0$  and  $(-\Delta S_{ads}^0)$  are respectively the intercept and the slope of the straight line obtained by plotting  $\Delta G_{ads}^0$  versus T (**Figure 5**).

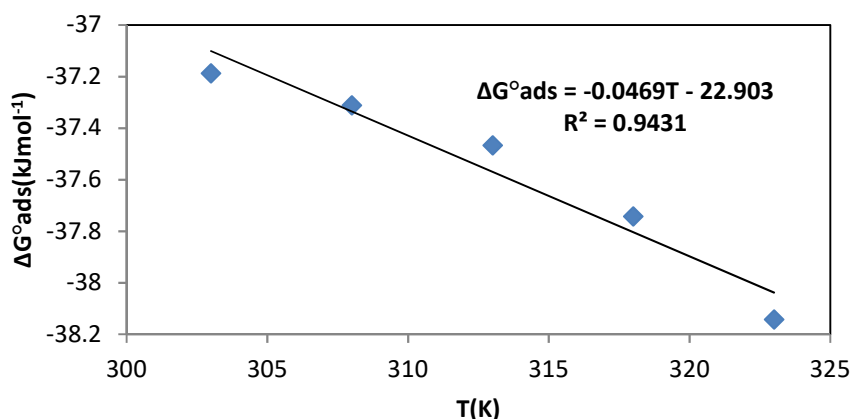


**Fig. 5.  $\Delta G_{ads}^0$  versus T for the adsorption of cefpodoxime on copper in 1M HNO<sub>3</sub>.**

3.4 EFFECT OF TEMPERATURE AND THERMODYNAMIC ACTIVATION PARAMETERS

**Figure 6** and **Figure 7** show respectively the plots  $\log W$  and  $\log(W/T)$  versus  $1/T$ .

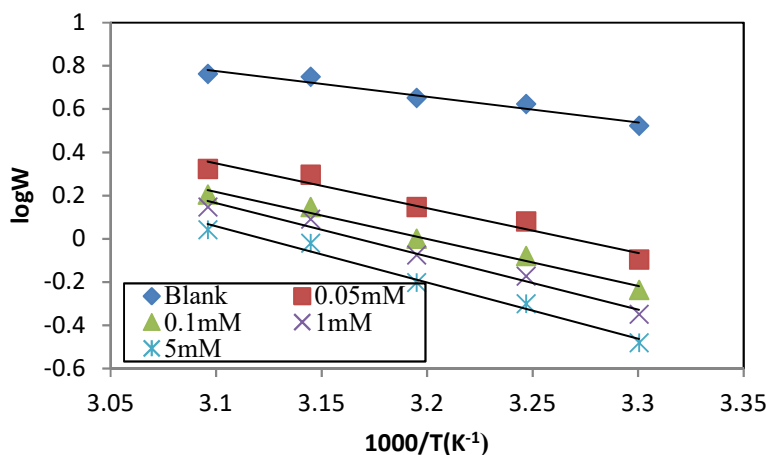


**Fig. 6. Arrhenius plots for Copper corrosion in 1M HNO<sub>3</sub> solutions without and with cefpodoxime**

All graphs show, both in absence and presence of cefpodoxime excellent linearity as expected from equations (22) and (23) respectively. The intercepts of the lines in **Figure 6** allow the calculation of the values of the pre-exponential factor ( $k$ ) and the slopes ( $-\frac{E_a}{2.303R}$ ) lead to the determination of the activation energy  $E_a$  both in the absence and presence of the inhibitor.

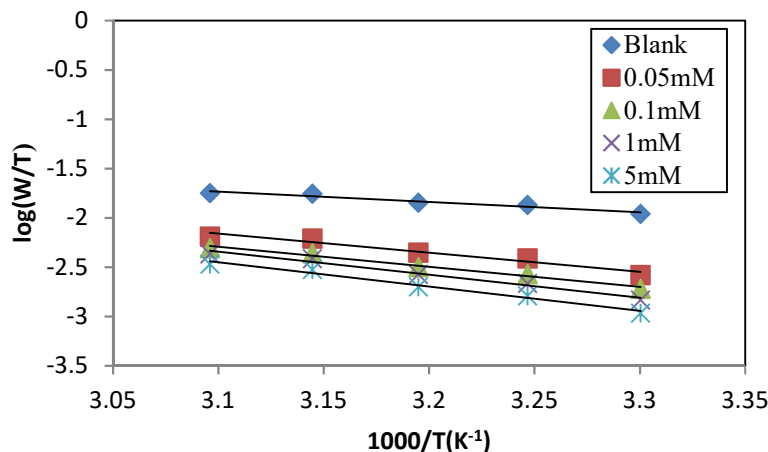


**Fig. 7.** Transition state plots for copper corrosion in 1M HNO<sub>3</sub> with or without cefpodoxime

The straight lines obtained by plotting  $\log(W/T)$  versus  $1/T$  (**Figure 7**) have a slope of ( $-\frac{\Delta H_a^*}{2.303R}$ ) and an intercept of  $[\log(\frac{R}{kR}) + \frac{\Delta S_a^*}{2.303R}]$ . Therefore, the values of  $\Delta H_a^*$  and  $\Delta S_a^*$  were calculated and displayed in **Table 3**

**Table 3.** Activation parameters for copper corrosion without and with cefpodoxime in 1M HNO<sub>3</sub>

	$E_a$ (kJmol <sup>-1</sup> )	$\Delta H_a^*$ (kJmol <sup>-1</sup> )	$\Delta S_a^*$ (Jmol <sup>-1</sup> K <sup>-1</sup> )
Blank	22.77	20.15	-167.87
0.05mM	39.65	37.00	-123.80
0.1mM	41.59	38.94	-120.31
1mM	47.15	44.49	-104.08
5mM	59.73	47.07	-98.14

### 3.5 SURFACE STUDIES

In order to characterize the metal surface behavior in contact with nitric acid solution in the absence and presence of the studied inhibitor, a surface analysis was carried out using scanning electron microscope, immediately after the corrosion tests. The copper samples in 1M HNO<sub>3</sub> solution with and without optimal concentration of the cefpodoxime drug were subjected to analysis. SEM images are shown in **Figure 8 A–C**.

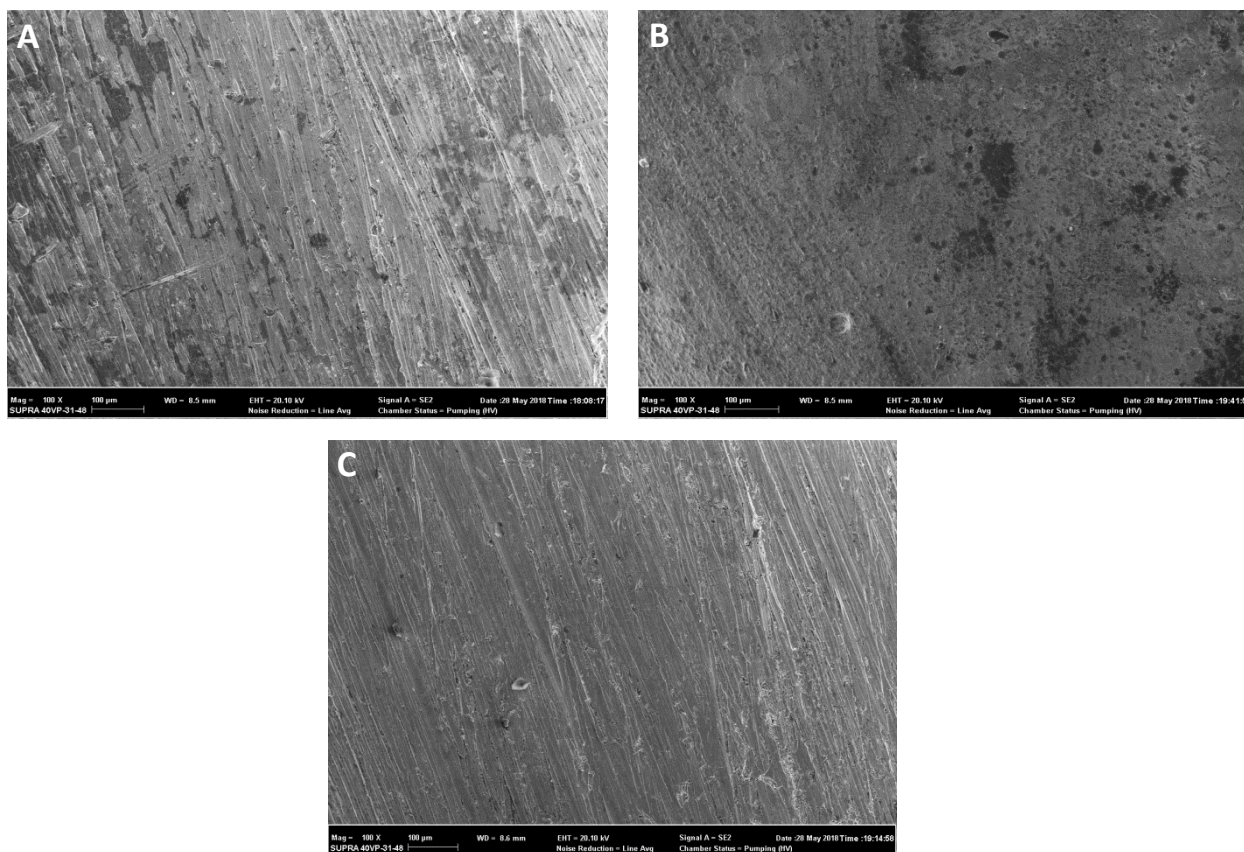


**Fig. 8. micrographs**

Micrographs show that surface corrosion of copper decreased remarkably in the presence of the inhibitor (**Figure 8-C**). Inspections of the figures reveal that there is severe damage, clear pits and cavities on the surface of copper in the absence of inhibitor (**Figure 8-B**) than in its presence and polished metal (**Figure 8-A**). There are fewer pits and cracks observed in the inhibited surface. It confirms that the metal surface is fully covered with the inhibitor molecules and a protective inhibitor film was formed.

### 3.6 QUANTUM CHEMISTRY CALCULATIONS

#### 3.6.1 GLOBAL REACTIVITY

In **Table 4**, we list the values of selected quantum chemical parameters calculated for the studied molecule by using DFT methods.

**Table 4. Molecular and reactivity descriptors of cefpodoxime**

Descriptor	Value	Descriptor	Value
$E_{\text{HOMO}}$ (eV)	-4.2110	$I$ (eV)	4.2110
$E_{\text{LUMO}}$ (eV)	-1.6417	$A$ (eV)	1.6417
$\Delta E$ (eV)	2.5693	$\mu$ (Debye)	9.0641
$\Delta N$	0.7992	$\eta$ (eV)	1.2847
$S$ (eV) <sup>-1</sup>	0.7784	$\omega$	3.3330
$\chi$ (eV)	2.9264	TE (a.u)	-2103.0911

HOMO and LUMO diagrams of the inhibitor are presented in **Figure 9**.

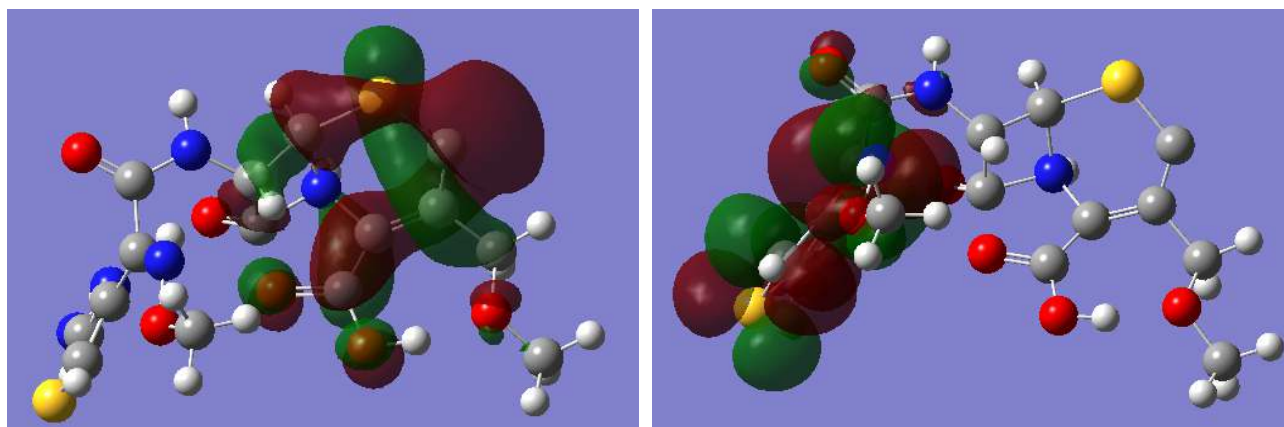


Fig. 9. HOMO (left) and LUMO (right) of cefpodoxime by B3LYP 6-31 G (d, p)

From Figure 9, it can be seen that the HOMO and LUMO diagrams of the studied molecule clearly present the active areas where transfers of electrons could occur (from the molecule to copper or vice-versa).

### 3.6.2 LOCAL REACTIVITY

The calculated Mulliken atomic charges, Fukui functions local softness indices by DFT at the B3LYP/6-31G (d, p) level are displayed in Table 5.

Table 5. Charges of some selected atoms, condensed Fukui functions and local softness indices

Atom	$q_k(N+1)$	$q_k(N)$	$q_k(N-1)$	$f_k^+$	$f_k^-$	$s_k^+$	$s_k^-$
C (1)	0.336	0.321	0.247	0.015	0.074	0.012	0.058
C (2)	0.379	0.377	0.279	0.002	0.098	0.002	0.076
C (3)	-0.420	-0.324	-0.307	-0.096	-0.017	-0.075	-0.013
S (4)	0.211	0.261	0.455	-0.050	-0.194	-0.039	-0.151
N (7)	-0.544	-0.580	-0.461	0.036	-0.119	0.028	-0.093
N (8)	-0.629	-0.617	-0.576	-0.012	-0.041	-0.009	-0.032
C (11)	0.135	0.144	0.269	-0.009	-0.125	-0.007	-0.097
C (12)	0.486	0.543	0.519	-0.057	0.024	-0.044	0.019
O (13)	-0.504	-0.472	-0.388	-0.032	-0.084	-0.025	-0.065
N (14)	-0.282	-0.186	-0.154	-0.096	-0.032	-0.075	-0.025
O (15)	-0.410	-0.389	-0.376	-0.021	-0.013	-0.016	-0.010
C (16)	-0.020	-0.057	-0.087	0.037	0.030	0.029	0.023
N (20)	-0.605	-0.512	-0.582	-0.093	0.070	-0.072	0.054
C (22)	-0.004	0.060	-0.012	-0.064	0.072	-0.050	0.056
<b>C (23)</b>	-0.064	-0.139	-0.138	<b>0.075</b>	-0.001	<b>0.058</b>	-0.001
C (27)	0.624	0.655	0.527	-0.031	0.128	-0.024	0.100
O (28)	-0.543	-0.581	-0.370	0.038	-0.211	0.030	-0.164
N (29)	-0.557	-0.519	-0.491	-0.038	-0.028	-0.030	-0.022
S (30)	-0.011	0.097	0.208	-0.108	-0.111	-0.084	-0.086
C (31)	-0.354	-0.283	-0.307	-0.071	0.024	-0.055	0.019
C (32)	-0.047	-0.070	0.057	0.023	-0.127	0.018	-0.099
C (33)	0.096	0.061	0.052	0.035	0.009	0.027	0.007
C (34)	0.445	0.541	0.600	-0.096	-0.059	-0.075	-0.046
O (35)	-0.463	-0.494	-0.475	0.031	-0.019	0.024	-0.015
O (36)	-0.576	-0.552	-0.531	-0.024	-0.021	-0.019	-0.016
C (38)	0.023	0.033	-0.135	-0.010	0.168	-0.008	0.131
O (39)	-0.512	-0.527	-0.431	0.015	-0.096	0.012	-0.075
<b>C (40)</b>	-0.045	-0.063	-0.248	0.018	<b>0.185</b>	0.014	<b>0.144</b>

## 4 DISCUSSION

### 4.1 CORROSION RATE VERSUS TEMPERATURE

The evolution of the corrosion rate for each concentration of cefpodoxime (**Figure 2**) shows a significant decrease in corrosion rate upon the addition of the studied inhibitor to the acidic solution, revealing the effectiveness of the molecule as a corrosion inhibitor for copper in 1 M nitric acid. A plausible explanation of these results is that the increasing inhibitor's concentration reduces the metal exposed surface to the corrosive environment through the increasing number of adsorbed molecules on its surface which hinders the direct acid attack on the metal surface [24].

### 4.2 INHIBITION EFFICIENCY VERSUS TEMPERATURE

As seen in **Figure 3**, inhibition efficiency decreases as the temperature increases for the concentration range studied. The literature [25] stated that decrease in inhibition efficiency with increase in temperature indicates physisorption of inhibitor on the corroding metal surface.

### 4.3 ADSORPTION MODEL

From the correlation coefficients ( $R^2$ ) and the slopes displayed in **Table 1**, the correlation coefficients are very close to unity and the slopes are also close to unity. Therefore, the studied inhibitor adsorbs on copper surface through Langmuir isotherm model.

### 4.4 ADSORPTION THERMODYNAMIC FUNCTIONS

Langmuir adsorption isotherm is described by Equation 19:

$$\frac{C_{inh}}{\theta} = \frac{1}{K_{ads}} + C_{inh} \quad (19)$$

where  $C_{inh}$  is the cefpodoxime concentration,  $K_{ads}$  is the equilibrium constant of thadsorption process and  $\theta$  is the degree of surface coverage. The equilibrium constant ( $K_{ads}$ ) is related to the standard free adsorption enthalpy by Equation 20 [26]:

$$\Delta G_{ads}^0 = -RT \ln(55.5K_{ads}) \quad (20)$$

In the above equation [27], 55.5 is the concentration of water in mol.  $L^{-1}$ ,  $T$  is the absolute temperature while  $R$  is the perfect gas constant. As displayed in **Table 2**, the obtained values of free adsorption enthalpy change,  $\Delta G_{ads}^0$  were negative, indicating the spontaneity of the adsorption process and the stability of the adsorbed layer [28] on the copper surface. It is generally accepted [26, 29] that values of  $\Delta G_{ads}^0$  around  $-40 \text{ kJ mol}^{-1}$  or more negative are associated with chemisorption while those of  $-20 \text{ kJ mol}^{-1}$  or less negative indicate physisorption. The values displayed in **Table 2** clearly indicate both chemisorption and physisorption. The standard adsorption enthalpy change  $\Delta H_{ads}^0$  and the standard adsorption entropy change  $\Delta S_{ads}^0$  are correlated with standard Gibbs free energy by Equation 21:

$$\Delta G_{ads}^0 = \Delta H_{ads}^0 - T\Delta S_{ads}^0 \quad (21)$$

In the present work,  $\Delta H_{ads}^0$  is negative, showing an exothermic process. The literature [30] revealed that an exothermic process means either physisorption or chemisorptions. Therefore this result confirms that the process of adsorption is both physisorption and chemisorption. The change in adsorption entropy ( $\Delta S_{ads}^0$ ) is positive, meaning that disorder increases during the adsorption process. This situation can be explained by the desorption of water molecules replaced by the inhibitor.

### 4.5 TEMPERATURE AND ACTIVATION PARAMETERS

Activation parameters are of great importance in the study of the inhibition mechanism of metals. The kinetics functions for the dissolution of copper without and with various concentrations of cefpodoxime are obtained by applying the Arrhenius equation and the transition state Equation 22-23 respectively:

$$\log W = \log k - \frac{E_a}{2.303RT} \quad (22)$$

$$\log \left( \frac{W}{T} \right) = \left[ \log \left( \frac{R}{kh} \right) + \frac{\Delta S_a^*}{2.303R} \right] - \frac{\Delta H_a^*}{2.303RT} \quad (23)$$

In these equations,  $E_a$  is the apparent effective activation energy,  $k$  is the Arrhenius pre-exponential factor;  $h$  is the Planck's constant,  $N$  is the Avogadro number,  $\Delta S_a^*$  is the change in activation entropy and  $\Delta H_a^*$  is the change in activation enthalpy.

According to the values displayed in **Table 3**, it seems that  $E_a$  and  $\Delta H_a^*$  varied in the same way, probably due to the thermodynamic relation between them ( $\Delta H_a^* = E_a - RT$ ). The higher values of effective activation energy ( $E_a$ ) in the presence of inhibitor as compared to the ( $E_a$ ) in the absence of inhibitor in the hydrochloric acid medium indicates that the inhibitor induces the energy barrier for the corrosion reaction which leads to the decreasing of rate of corrosion of copper in the presence of inhibitor [28]. Furthermore, the inhibition efficiencies decrease with the increase in temperature. This trend in the evolution of the activation energy  $E_a$  can be interpreted as an indication for physical adsorption [31]. The value of  $\Delta H_a^*$  is higher for inhibited solution than that for the uninhibited solution. This suggested that an increase in randomness occurred on going from reactants to the activated complex. This might be results of the adsorption of cefpodoxime molecules from the acid solution could be regarded as quasi-substitution between the cefpodoxime in the aqueous phase and water molecules on copper surface. In such condition, the adsorption of inhibitor molecules was followed by desorption of water molecules from the copper surface. Thus increase in entropy of activation was attributed to solvent ( $H_2O$ ) entropy [32].

## 4.6 QUANTUM CHEMICAL CALCULATIONS

### 4.6.1 GLOBAL PARAMETERS

Quantum chemical parameters obtained from the calculations which are responsible for the inhibition efficiency of given inhibitor such as the energies of frontier molecular orbitals ( $E_{HOMO}$ ) and ( $E_{LUMO}$ ), the separation energy ( $E_{LUMO}-E_{HOMO}$ ),  $\Delta E$ , representing the function of reactivity, the electron affinity, the ionization potential, dipole moment, total energy etc are collected in **Table 4**. The energy of the HOMO ( $E_{HOMO}$ ) represents the ability of a given molecule to donate a lone pair of electrons and the higher the  $E_{HOMO}$  value, the greater the tendency of the molecule to donate electrons to an electrophilic reagent [33] and the lower the  $E_{LUMO}$ , the greater the tendency of the molecule to accept electrons from metal atoms. Results from **Table 4** show that cefpodoxime has low  $E_{LUMO}$  and high  $E_{HOMO}$ . This high  $E_{HOMO}$  value indicates the tendency to donate electrons to empty molecular orbital of copper ions ( $Cu^{2+}$ :  $[Ar] 3d^9$ ). The energy difference between  $E_{HOMO}$  and  $E_{LUMO}$  (i.e.,  $\Delta E$ ) implies the more or less reactivity of the given compound; the smaller the  $\Delta E$  value, the greater the reactivity of the molecule. The results (see **Table 4**) show that the studied inhibitor has 2.5693 eV as separation energy. That could explain the high inhibition efficiency obtained (90.09%) for 5 mM of cefpodoxime at 303K.

The dipole moment gives information on the polarity. The higher the dipole moment, the higher is the polarity of the molecule [34]. As seen in **Table 4**, the dipole moment value is very high (9.0641Debye) compared with that of many other molecules. Many authors state that high values of dipole moment [35] probably leads to an important adsorption of the chemical compound on the metal surface and therefore higher inhibition efficiency.

The ionization potential ( $I$ ) and the electronic affinity ( $A$ ) are respectively (4.2110eV) and (1.6417 eV). This low value of ( $I$ ) and the high value of electron affinity indicate the capacity of the molecule both to donate and accept electron. The electronegativity ( $\chi$ ) indicates the capacity of a compound to attract electrons; whereas the hardness ( $\eta$ ) expresses the degree of reactivity of the system (low values of hardness indicate a tendency to donate electrons). In our work the low value of the electronegativity of the studied molecule when compared to that of copper and the low value of hardness (1.2847eV) confirm the relatively higher value of the fraction of electrons transferred ( $\Delta N = 0.7992$ ). The electrophilicity index measures the propensity of chemical species to accept electrons; a high value of electrophilicity index describes a good electrophile while a small value of electrophilicity index describes a good nucleophile. In this work the obtained value ( $\omega = 3.3330eV$ ) shows the good capacity of cefpodoxime to accept electrons.

### 4.6.2 LOCAL PARAMETERS

Local reactivity descriptors including Fukui functions and local softness indices were collected in **Table 5**.

The analysis of **Table 5** indicates that according to the Fukui theory of reactivity, C (23) is the nucleophilic attacks center ( $f_k^+$  is maximum) when C (40) is the electrophilic attacks center ( $f_k^-$  is maximum). The local softness contains the information similar to those condensed Fukui function plus additional information about the total molecular softness. A high value of  $s_k^+$  indicates high nucleophilicity and the high value of  $s_k^-$  indicates high electrophilicity.

## 5 CONCLUSION

Cefpodoxime drug shows good inhibition properties for copper corrosion in 1 M HNO<sub>3</sub>. The inhibition efficiency increases with increasing concentration in the studied inhibitor but decreases with rise in temperature. Adsorption of cefpodoxime follows the Langmuir adsorption isotherm. The adsorption and activation thermodynamic functions reveal a spontaneous adsorption process of the studied molecule onto copper and both physisorption and chemisorption mechanisms with predominance of physisorption. The SEM images confirm the formation of a protective layer on the metal surface. Quantum chemical calculations data from B3LYP/6-31G (d, p) are consistent with the experimental results.

## ACKNOWLEDGEMENTS

The authors are grateful to the Laboratory of Physical Chemistry of Félix Houphouët-Boigny University of Cocody-Abidjan.

## REFERENCES

- [1] M. Vincent, P. Hartemann, and M. Engels-Deutsch, "Antimicrobial applications of copper," *International Journal of Hygiene and Environmental Health*, vol. 219, no. 7, pp. 585-591, 2016.
- [2] X. Liu, and D. Astruc, "Atomically precise copper nanoclusters and their applications," *Coordination Chemistry Review*, vol. 359, pp. 112-126, 2018.
- [3] O. A. Hazazi, and M. Abdallah, "Prazole compounds as inhibitors for corrosion of aluminum in hydrochloric acid," *International Journal of Electrochemical Science*, vol. 8, pp. 8138-8152, 2013.
- [4] M. N. El-Haddad, and A. S. Fouda, "Electroanalytical, quantum and surface characterization studies on imidazole derivatives as corrosion inhibitors for aluminum in acidic media," *Journal of Molecular Liquids*, vol. 209, pp. 480-486, 2015.
- [5] M. Abdallah, "Antibacterial drugs as corrosion inhibitors for corrosion of aluminium in hydrochloric solution," *Corros. Sci.*, vol. 46, no. 8, pp. 1981-1996, 2004.
- [6] G. Gece, "The use of quantum chemical methods in corrosion inhibitor studies" *Corrosion Science*, vol. 50, no. 11, pp. 2981-2992, 2008.
- [7] I. B. Obot, N. O. Obi-Egbedi, and S. A. Umoren, "The synergistic inhibitive effect and some quantum chemical parameters of 2,3-diaminonaphthalene and iodide ions on the hydrochloric acid corrosion of aluminium," *Corrosion Science*, vol. 51, no. 2, pp. 276-282, 2009.
- [8] S. M. A. E. Haleem, S. A. E. Wanees, E. E. A. E. Aal, and A. Farouk, "Factors affecting the corrosion behaviour of aluminium in acid solutions. I. Nitrogen and/or sulphur-containing organic compounds as corrosion inhibitors for Al in HCl solutions," *Corrosion Science*, vol. 68, pp. 1-13, 2013.
- [9] K. F. Khaled, and M. M. Al-Qahtani, "The inhibitive effect of some tetrazole derivatives towards Al corrosion in acid solution: Chemical, electrochemical and theoretical studies" *Material Chemistry and Physics*, vol. 113, pp. 150-158, 2009.
- [10] Y. Xiao-Ci, Z. Hong, L. Ming-Dao, R. Hong-Xuan, and Y. Lu-An, "Quantum chemical study of the inhibition properties of pyridine and its derivatives at an aluminum surface," *Corrosion Science*, vol. 42, no. 4, pp. 649-653, 2000.
- [11] E. S. H. E. Ashry, A. E. Nemr, S. A. Esawy, and S. Ragab, "Corrosion inhibitors - Part II: Quantum chemical studies on the corrosion inhibitions of steel in acidic medium by some triazole, oxadiazole and thiadiazole derivatives," *Electrochimica Acta*, vol. 51, no. 19, pp. 3957-3968, 2006.
- [12] M. J. Frisch, G. W. Trucks, G. E. S. H. B. Schlegel, M. A. Robb, J. R. Cheeseman, G. Scalmani, V. Barone, B. Mennucci, G. A. Petersson, H. Nakatsuji, M. Caricato, X. Li, H. P. Hratchian, A. F. Izmaylov, J. Bloino, G. Zheng, J. L. Sonnenberg, M. Hada, M. Ehara, K. Toyota, R. Fukuda, J. Hasegawa, M. Ishida, T. Nakajima, Y. Honda, O. Kitao, H. Nakai, T. Vreven, J. A. Montgomery, Jr., J. E. Peralta, F. Ogliaro, M. Bearpark, J. J. Heyd, E. Brothers, , and V. N. S. K. N. Kudin, R. Kobayashi, J. Normand, K. Raghavachari, A. Rendell, J. C. Burant, S. S. Iyengar, J. Tomasi, M. Cossi, N. Rega, J. M. Millam, M. Klene, J. E. Knox, J. B. Cross, V. Bakken, C. Adamo, J. Jaramillo, R. Gomperts, R. E. Stratmann, O. Yazyev, A. J. Austin, R. Cammi, C. Pomelli, J. W. Ochterski, R. L. Martin, K. Morokuma, V. G. Zakrzewski, G. A. Voth, P. Salvador, J. J. Dannenberg, S. Dapprich, A. D. Daniels, O. Farkas, J. B. Foresman, J. V. Ortiz, J. Cioslowski, and D. J. Fox, , pp. Gaussian 09, Revision A.02, Gaussian, Inc., Wallingford CT, 2009.
- [13] A. D. Becke, "Density Functional thermochemistry. III. The role of exact exchange," *Journal of Chemical Physics*, vol. 98, no. 7, pp. 5648-5652, 1993.
- [14] C. Lee, W. Yang, and R. G. Parr, "Development of the Colle Salvetti correlation-energy formula into a functional of the electron density," *Physical Review B*, vol. 37, no. 2, pp. 785-789, 1988.
- [15] B. Miehlich, A. Savin, H. Stoll, and H. Preuss, "Results obtained with the correlation energy density functionals of Becke and Lee, Yang and Parr," *Chemical Physics Letters*, vol. 157, no. 3, pp. 200-206, 1989.

- [16] S. G. Zhang, W. Lei, M. Z. Xia, and F. Y. Wang, "QSAR study on N-containing corrosion inhibitors: Quantum Chemical approach assisted by topological index," *Journal of Molecular Structure : THEOCHEM*, vol. 732, no. 1-3, pp. 173-182, 2005.
- [17] T. Koopmans, "Über die Zuordnung von Wellenfunktionen und Eigenwerten zu den Einzelnen Elektronen Eines Atoms," *Physica*, vol. 1, no. 1-6, pp. 104-113, 1934.
- [18] R. G. Pearson, "Absolute electronegativity and hardness: application to inorganic chemistry," *Inorganic Chemistry*, vol. 27, no. 4, pp. 734-740, 1988.
- [19] R. G. Parr, L. V. Szentpaly, and S. Liu, "Electrophilicity index," *Journal of the American Chemical Society*, vol. 121, no. 9, pp. 1922-1924, 1999.
- [20] E. E. Ebenso, T. Arslan, F. Kandemirli, I. N. Caner, and I. I. Love, "Quantum Chemical Studies of some Rhodamine Azosulpha Drugs as corrosion inhibitors for mild steel in Acidic Medium," *International Journal of Quantum Chemistry*, vol. 110, no. 5, pp. 1003-1018, 2010.
- [21] P. Fuentealba, P. Perez, and R. Contreras, "On the condensed Fukui function," *Journal of Chemical Physics*, vol. 113, no. 7, pp. 2544-2551, 2000.
- [22] M. A. Quijano, M. Palomar-Pardavé, A. Cuan, M. R. Romo, G. N. Silva, R. A. Bustamante, A. R. Lopez, and H. H. Hernandez, "Quantum Chemical Study of 2-Mercaptoimidazole, 2-Mercaptobenzimidazole, 2-Mercapto-5-Methylbenzimidazole and 2-Mercapto-5-Nitrobenzimidazole as Corrosion Inhibitors for Steel" *International Journal of Electrochemical Science*, vol. 6, pp. 3729-3742, 2011.
- [23] W. Yang, and W. J. Mortier, "The use of global and local molecular parameters for the analysis of the gas-phase basicity of amines," *Journal of the American Chemical Society*, vol. 108, no. 19, pp. 5708-5711, 1986.
- [24] N. Y. S. DIKI, K. V. BOHOUSOU, M. G.-R. KONE, A. OUEDRAOGO, and A. TROKOUREY., "Cefadroxil Drug as Corrosion Inhibitor for Aluminum in 1 M HCl Medium: Experimental and Theoretical Studies," *IOSR Journal of Applied Chemistry*, vol. 11, no. 4, pp. 24-36, 2018.
- [25] R. Saratha, and R. Meenakshi, "Corrosion inhibitor: A plant extract," *Der Pharma Chemica*, vol. 2, no. 1, pp. 287-294, 2010.
- [26] H. Keles, M. Keles, I. Dehri, and O. Serinday, "Adsorption and inhibitive properties of aminobiphenyl and its Schiff base on mild steel corrosion in 0.5 M HCl medium," *Colloids Surfaces A: Physicochemical and Engineering Aspects*, vol. 320, no. 1-3, pp. 138-145, 2008.
- [27] R. F. V. Villamil, P. Corio, J. C. Rubin, and S. M. L. Agostinho, "Effect of sodium dodecylsulfate on copper corrosion in sulfuric acid media in the absence and presence of benzotriazole," *Journal of Electroanalytical Chemistry*, vol. 472, pp. 112-116, 1999.
- [28] M. R. Singh, K. Bhrara, and G. Singh, "The Inhibitory Effect of Diethanolamine on Corrosion of Mild Steel in 0.5 M Sulphuric Acidic Medium," *Portugaliae Electrochimica Acta*, vol. 26, no. 6, pp. 479-492, 2008.
- [29] S. Issadi, T. Douadi, A. Zouaoui, S. Chafaa, M. A. Khan, and G. Bouet, "Novel Thiophene symmetrical Schiff base compounds as corrosion inhibitor for mild steel in acidic media," *Corrosion Science*, vol. 53, no. 4, pp. 1484-1488, 2011.
- [30] W. Durnie, R. D. Marco, A. Jefferson, and B. Kinsella, "Development of a Structure-Activity Relationship for Oil Field Corrosion Inhibitors," *Journal of Electrochemical Society*, vol. 146, no. 5, pp. 1751-1756, 1999.
- [31] A. K. Singh, and M. A. Quraishi, "Investigation of adsorption of isoniazid derivatives at mild steel/hydrochloric acid interface: Electrochemical and weight loss methods," *Material Chemistry and Physics*, vol. 123, no. 2-3, pp. 666-677, 2010.
- [32] D. K. Yadav, and M. A. Quraishi, "Application of some condensed uracils as corrosion inhibitors for mild steel: gravimetric, electrochemical, surface morphological, UV-visible and theoretical investigations," *Industrial and Engineering Chemistry Research*, vol. 51, pp. 14966-14979, 2012.
- [33] M. Özcan, I. Dehri, and M. Erbil, "Organic sulphur-containing compounds as corrosion inhibitors for mild steel in acidic media: correlation between inhibition efficiency and chemical structure," *Applied Surface Science*, vol. 236, no. 1-4, pp. 155-164, 2004.
- [34] N. O. Eddy, F. E. Awe, C. E. Gimba, N. O. Ibsi, and E. E. Ebenso, "QSAR, Experimental and Computational Chemistry Simulation Studies on the Inhibition Potentials of Some Amino Acids for the Corrosion of Mild Steel in 0.1 M HCl," *International Journal of Electrochemical Science*, vol. 6, no. 931-957, pp. 931, 2011.
- [35] N. Khalil, "Quantum chemical approach of corrosion inhibition," *Electrochimica Acta*, vol. 48, no. 18, pp. 2635-2640, 2003.